Proceedings of the ASME 2017 International Technical Conference and Exhibition on Packaging and Integration of Electronic and Photonic Microsystems
InterPACK2017
August 29-September 1, 2017, San Francisco, California, USA

IPACK2017-74339

IMPACT OF TILE DESIGN ON THERMAL PERFORMANCE OF OPEN AND ENCLOSED AISLES

Sadegh Khalili
State University of New York at Binghamton-SUNY
Binghamton, NY, USA

Mohammad I. Tradat
State University of New York at Binghamton-SUNY
Binghamton, NY, USA

Kourosh Nemati
Future Facilities Ltd.
San Jose, CA, USA

Mark Seymour
Future Facilities Ltd.
London, UK

Bahgat Sammakia
State University of New York at Binghamton-SUNY
Binghamton, NY, USA

ABSTRACT

In raised floor data centers, tiles with high open area ratio or complex understructure are used to fulfill the demand of today's high-density computing. Using more open tiles reduces pressure drop across the raised floor with the potential advantages of increased airflow and lower noise. However, it introduces the disadvantage of increased non-uniformity of airflow distribution. In addition, there are various tile designs available on the market with different opening shapes or understructures. Furthermore, a physical separation of cold and hot aisles (containment) has been introduced to minimize the mixing of cold and hot air. In this study, three types of floor tiles with different open area, opening geometry, and understructure are considered. Experimentally validated detail models of tiles were implemented in CFD simulations to address the impact of tile design on the cooling of IT equipment in both open and enclosed aisle configurations. Also, impacts of under-cabinet leakage on the IT equipment inlet temperature in the provisioned and under-provisioned scenarios are studied. Finally, a predictive equation for the critical under-provisioning point that can lead to a no-flow condition in IT equipment with weaker airflow systems is presented.

NOMENCLATURE

CA	Cold Aisle
CAC	Cold Aisle Containment
CRAH	Computer Room Air Handler
GR	Geometrical Resolution
HA	Hot Aisle
IAT	Inlet Air Temperature
N	Number of IT units
OAT	Outlet Air Temperature
Q	Airflow rate (CFM)
SAT	Supplied Air Temperature
UCL	Under Cabinet Leakage

INTRODUCTION

A raised floor data center is a facility housing computer systems and associated components. Such facilities are commonly cooled using air supplied by the Computer Room Air Handler (CRAH) units to the IT equipment through perforated floor tiles. A perforated tile is supposed to supply a sufficient amount of cooled air to the adjacent rack or racks. The required airflow of the rack depends on the IT equipment heat dissipation, temperature of cooling air, and internal design of IT equipment. The thermal management of data centers has become more challenging as the rack-level power density has been increased. This increase in power density means that more cooled air is needed to dissipate the generated heat from IT equipment. Therefore, tiles with a higher open area ratio and/or complex understructure are used to maximize airflow delivery to any adjacent high-density racks. In a raised floor data center, the plenum pressure, airflow rate through tiles, and airflow pattern inside the aisles depend on the geometrical features of the tiles such as porosity, size and shape of openings, solid margin around tile, and the presence of understructure scoops, guiding fins, or dampers. Therefore, the perforated floor tiles are complex components of a data center that play a key role in the cooling performance of it.

Many numerical and experimental studies have been done investigating airflow through perforated tiles. Kang et al. [1] proposed to use a Flow Network Modeling (FNM) approach for the prediction of the distribution of flow rates exiting from various tiles. Schmidt et al. [2] presented a predictive model for the airflow distribution through tiles for various tile layouts and operations scenarios for the air conditioning units. VanGilder and Schmidt [3] studied the relation between tile airflow uniformity and parameters such as perforated tile type, floor plan, plenum obstructions, plenum depth, and airflow leakage rate. Ling et al. [4] studied the impact of geometrical factors and flow parameters on the pressure loss coefficient across perforated tiles and proposed a fitting equation for the pressure loss coefficient. Arghode et al. [5] investigated the shortcomings of available commercial airflow measurement tools and introduced two other methods for tile airflow rate measurement. The first tool utilizes an array of thermal anemometers while the second works based on calorimetry principles.

As the complexity of the cooling of data centers has increased, computational fluid dynamics (CFD) has emerged as a tool for the design of data centers cooling. CFD allows architects and engineers to evaluate several options for planning, air conditioning, piping, and wiring, and try alternate approaches before a physical implementation. Furthermore, CFD can be used for evaluation and optimization of an existing data center. Engineers can predict performance for potentially dangerous situations, such as a cooling failure or sudden change in cooling demand. In addition, engineers may find out what the benefits and/or potential cooling problems of a reconfiguration of the data center are by performing CFD simulations. This enables them to avoid poor decisions, and adopt strategies that facilitate good performance.

The accuracy of the results of a CFD simulation depends on how accurately the details are captured. Due to limits of computational resources, a very detailed modeling of facilities is computationally expensive or perhaps not possible in some cases. Instead, many commercial CFD software packages utilize simplified (compact) models of objects to reduce computation costs. Therefore, the accuracy of the results is highly dependent on the performance of CFD compact models. Consequently, researchers started focusing on developing CFD models of perforated floor tiles. One of the earliest suggested models considers the tile as a porous medium and assumes a step pressure loss across the tile surface (known as "porous jump model") [6-8]. Even though this model can predict airflow rates of tiles with an acceptable accuracy, it neglects changes in the momentum of air as it transfers across the tile. Therefore, the porous jump model fails to capture effects of ambient air entrainment and by-pass of air from the top of the rack. Abdelmaksoud et al. [9] proposed an improved model by adding a momentum source in a region with the same width and length as the tile perforated area at a preselected height above the tile surface to capture the effect of the momentum rise of air (known as "body force model"). Arghode et al. [10] suggested a modification for the body force model that uses velocity at the jet vena contracta instead of average pore velocity that was used in the original body force model for calculating the momentum rise. Recently, Arghode and Joshi [11] analyzed momentum-source region dimensions to include the effects of open area ratio, size of openings, and solid edges of tiles.

In an open aisle configuration, jets of cold air (from the CRAH units) with high momentum from perforated tiles can by-pass the IT equipment over the tops of racks and mix with warm IT exhaust air, which decreases thermodynamic efficiency of the data center. In recent years, a physical barrier between hot and cold aisles has been suggested as an important energy-saving strategy to minimize the mixing of hot and cold air [12]. It has been found that implementation of a cold aisle containment (CAC) can save up to 40% on cooling energy [13, 14]. Muralidharan et al. [14] studied the impact of CAC on overall data center efficiency. Makwana et al. [15] discussed the benefits of sealing a CAC system by blanking panels and grommets. Alissa et al. [16], as well as Shrivastava and Ibrahim [17], investigated cooling failure in CAC systems.

A common belief is that the type of tile is not an important factor in a CAC system. In this study, the impacts of tile design on the thermal performance of open and enclosed aisle configurations is investigated and discussed. Three types of tiles with different openness, opening geometry, and understructure design are considered. To the best of the authors' knowledge, in all the previous studies on the CFD modeling of perforated tiles, air was assumed to approach the tile normal to its surface, which is an inaccurate assumption [18]. Therefore, experimentally validated geometrical resolution (GR) model of tiles are used for the CFD simulations undertaken with the data center-specific 6SigmaRoom application in this study. The airflow rate and temperature at the inlet of servers, under-cabinet leakages, and possible locations of hot spots with and without a CAC system for neutrally provisioned and under-provisioned cases are reported for the three different types of tiles shown in Fig. 1.

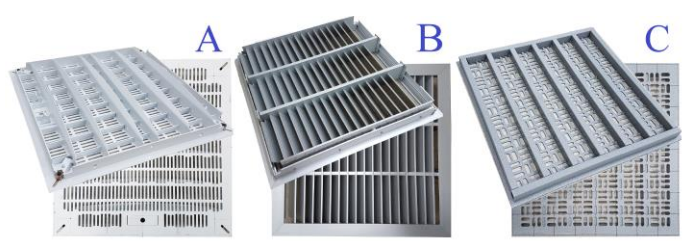

Figure 1. Tiles under investigation.

CFD MODELING

Three different types of tile with various openness, opening geometry, and understructure were considered for this study as shown in Fig. 1. Tile A is a slotted grill with parallel openings and understructure scoops. The scoops are claimed to increase the air pickup from the plenum. Tile B is a directional grill with 77 mm long vanes that are angled 55.7° from the surface of the tile. The directional tiles are designed to be installed so as to angle air towards equipment to increase the capture index. The capture index is defined as the ratio of airflow entering the face of the rack to the total airflow of the tile. Tile C has a simple understructure design, and perpendicular openings on its surface. The ratio of open area to total surface area (openness ratio) of tiles A, B and C were calculated as 30.4%, 58%, and 35.3%, respectively.

Recently, Khalili et al. [18] experimentally showed that different directions of approaching flow to a perforated floor tile can lead to different flow field developments downstream of the tile. Previous CFD characterization studies of perforated tiles were based on the assumption that air approaches from a normal direction to the surface of the tile (see [9-11]). The CFD results of the airflow field above a GR model of tile A and an available compact model of a slotted tile are compared in Fig. 2. The GR model is a detailed model of the tile that was built using a CAD software and imported to 6SigmaRoom to geometrically resolve structural details of the tile. Experimental flow visualization data above the same type of tile is also presented in Fig. 2a that shows good agreement between the direction of jets above the tile in the CFD simulation using the GR model and the experiment. The two vertical red lines in the experimental image indicate the location of the tile edges. The airflow rate through the GR and compact models of tile A are presented in Fig. 2, and was measured as 709 CFM experimentally with similar boundary conditions (see [18] for details of the experimental setup and results). The implemented compact model imposes a body force on the flow to capture the effect of the momentum rise of the air jets. This compact model is the simplified approach commonly used where no additional key geometry is added to reflect specifics of the tile. The direction and width of the slots, and the open area of the tile were specified and the directionality of the slots was set to normal. This compact model has the option of straightening flow that only transfers the normal momentum and results in a flow normal to the surface of the tile. With the flow-straightening option set to be off, the tangential momentum in the direction of the slots completely transfers across the tile and does not drop. Figure 2a shows that the direction of jets of air in the GR model is consistent with the experimental visualizations, while this direction is different downstream of the compact model (Fig. 2b). Thus, in order to have more reliable results, GR models were used in this study. It should be mentioned that the compact model was able to predict the airflow rate with an acceptable accuracy (about 1% error).

A typical data center cell, as shown in Fig. 3, was considered for CFD simulation. The total area of the cell is 65.4 m^2 (704 sq.ft.) with a 0.91 m (3 ft) deep plenum and 4.37 m (14.3 ft) ceiling height. A total of 28 perforated floor tiles, each 0.61 m × 0.61 m (2 ft × 2 ft), was distributed in the aisle in two rows. The aisle has two cabinet rows with a total of 24 racks. The racks' overall dimensions are 710 mm × 1065 mm × 2114 mm. Each rack was populated by twenty 2 RU servers and one network switch, and was recessed by 30 mm from the tile edge. The cabinet was populated by DELL PowerEdge 2950 server models. The power consumption of the server was characterized experimentally. At 100% CPU utilization when the fans were operating at maximum RPM, each server consumes about 387 W. Therefore, the power consumption was set at this value in the numerical model. The generated heat was assumed to be fully convected by the cooling air (no conduction heat transfer to the rack frame or radiation to other cooler objects). The switches have a nameplate power of 118 W and were operating at a heat power factor of 50%. In 6SigmaRoom, the power factor reduces the power of IT equipment to a more realistic level, as the name plate power is often a significant over-estimation of the heat dissipation in normal operation. The empty slots were blocked by blanking panels and the cabinet leakage area was set to zero (e.g. no cabinet leakage). The gap between the rack and floor, resulting from 38 mm legs of the rack, was considered as the only source of leakage (known as UCL). The network switches were mounted to the front rack flanges with their inlet faced to the cold aisle. The numbering system is shown in Fig. 3.

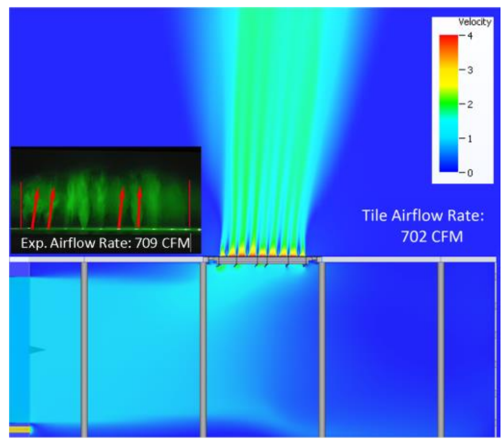

(a)

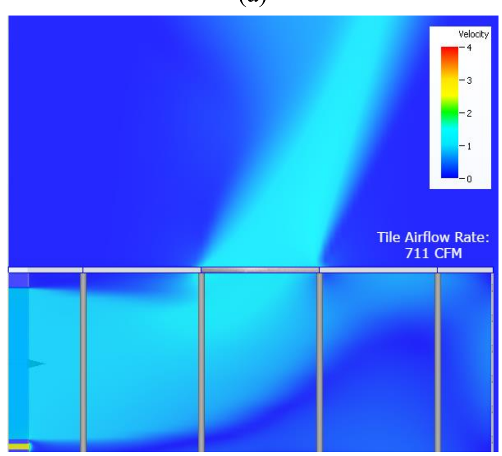

(b)

Figure 2. (a) Numerical result with GR model of tile A (experimental flow visualization data is from [18]), (b) Numerical results with an available CFD model for slotted tiles with the same open area as tile A.

A pressure-dependent boundary condition was assigned on the outlet of each IT equipment unit. This boundary condition was extracted experimentally, and accurately describes the airflow rate through the IT equipment (see [19, 22]). This boundary condition adjusts the airflow through the equipment based on the differential pressure between the inlet and outlet of the unit. Alissa et al. [19] built a CFD model of the data center laboratory at the Binghamton University ES2 center using the pressure-dependent boundary condition. They successfully validated the CFD model by performing experiments with various scenarios.

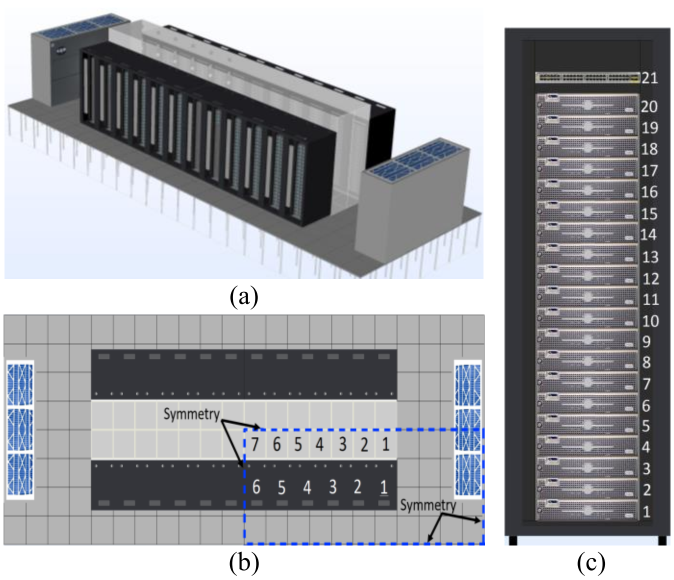

Figure 3. (a) 3D map of the data center cell (b) Layout of the data center cell, (c) Numbering system of IT equipment.

Two perimeter downflow air conditioning units were deployed to supply a total airflow of 48000 CFM at 22 °C (71.6 °F) for provisioning the IT equipment. It should be mentioned that the ASHRAE recommends an air temperature range of 18-27 °C at the servers' inlet [20]. The CAC doors are located exactly at the beginning and end of the aisle, while the ceiling of containment was placed 37 cm above the top of the racks. Considering the symmetry of the layout, the cell can be divided into smaller regions with symmetry conditions on the walls as shown in Fig. 3b. In this study, the outlined area is considered and simulated. The mesh was refined in the regions of GR models to achieve the good number of minimum 32 cells/pore (8 cells/pore is the minimum recommended grid size by [21]).

RESULTS

In the present investigation, the open and CAC systems with and without under-cabinet leakage for provisioned and under-provisioned conditions in 6 different cases are examined. In cases 1 to 4, the supplied airflow was 12000 CFM when the required airflow for provisioning was 11971 CFM (based on the free delivery point of servers with fans at maximum RPM). This means that the equipment in the aisle was slightly over-provisioned by less than 30 CFM, which is negligible. In cases 1 and 2, the impact of tile design in an open aisle system with and without under-cabinet leakage is studied. In cases 3 and 4, a CAC system with entrance doors, side walls, and ceiling installed on the cold aisle (CA) is investigated. Finally, two under-provisioned scenarios (83% provisioning) are investigated in the CAC configuration with and without UCL in cases 5 and 6, respectively.

Case 1: Open aisle, with under-cabinet leakage

In this case, no containment is installed and hot air can leak from the hot aisle (HA) to the cold aisle (CA) through the open area both above and below the rack. These leakages lead to a mixing of hot and cold air that results in thermodynamic inefficiencies and under-utilization of available cooling resources. Figure 4 shows the variation of air temperature at the inlet of servers when tiles of type A are distributed in the aisle. It is seen that inlet air temperature (IAT) of the servers in rack 1 is much higher than the supplied air temperature (SAT). This is mainly due to the mixing of hot air with supplied cold air at the entrance of the aisle. Figure 4 also shows that the first two servers at the bottom of all the racks receive air with the highest inlet temperature in comparison with the rest of the servers in their respective racks. This high temperature is due to hot air leakage through the gap beneath the racks and its entrainment with the high velocity jets (up to 4 m/s) of air through the floor tiles. It is worth mentioning that this high velocity is due to the relatively small openings of tile A. Figure 4 also demonstrates that the first server at the bottom of rack 1 is exposed to the danger of overheating. This is because of hot air entrainment from entrance of the aisle and the under-cabinet gap. In addition, the temperature rise in the supplied air to servers 8-20 is less than 1.2 °C while this temperature rise is at least 3 °C for servers 1-4 (with a maximum 7.5 °C for server 1 in rack 1).

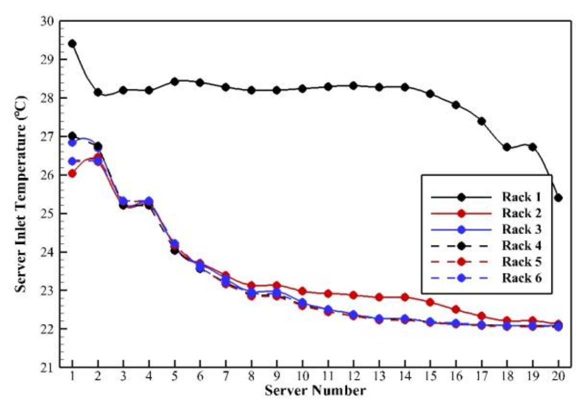

Figure 4. Air temperature at the inlet of servers with tiles of type A installed in the open aisle system, with UCL.

Figure 5 presents the variation of inlet air temperature when tiles of type B were installed. A significant decrease in the IAT is seen for the servers at the bottom half of the racks, while a temperature increase is seen at the inlet of servers at the top half of the racks. With tile B installed, the maximum air temperature rise from SAT at the inlet of servers in rack 1 is 4.2 °C when the IAT of servers for the rest of the racks remains within 2.5 °C of the SAT. The IAT drop for the servers at the bottom of the rack is due to the design of tile B that directs airflow toward the bottom-half of the rack. Figure 6 shows the IAT of servers when tiles of type C are installed. The variation of IAT shows a similar trend as the tiles of type A. The maximum difference between the IAT in the results of tiles A and C is 1.5 °C.

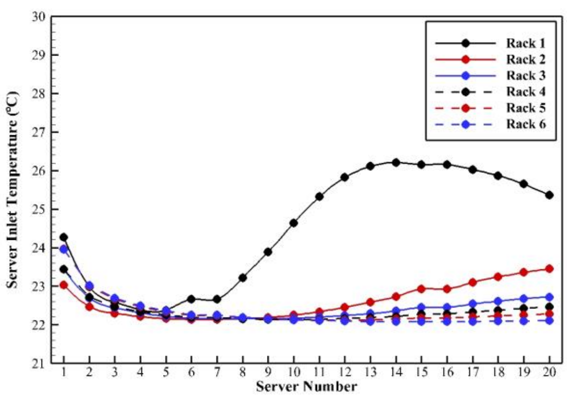

Figure 5. Air temperature at the inlet of servers with tiles of type B installed in the open aisle system, with UCL.

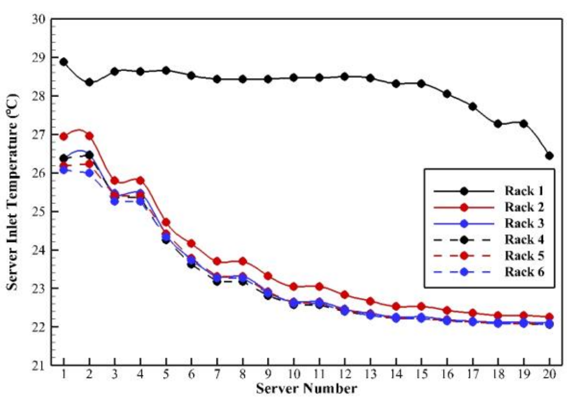

Figure 6. Air temperature at the inlet of servers with tiles of type C installed in the open aisle system, with UCL.

Case 2: Open aisle, without under-cabinet leakage

In this case, the gap underneath the racks is blocked and hot air can only leak into the cold aisle from above the racks and from the entrance of the aisle. The variations of IAT when tiles of type A, B, and C are distributed in the aisle are presented in Figs. 7-9, respectively. As we can see in Fig. 7, the IAT of servers in rack 1 are between 2.3 and 6.4 °C higher than the SAT, while the difference between IAT and SAT for the rest of the servers in other racks is less than 0.5 °C. This shows that a simple blockage of the under-cabinet gap can eliminate the risk of overheating in a large portion of IT equipment in an open aisle system. It should however be noted that the remainder of the rack is assumed to provide perfect segregation between hot and cold aisles and so some deterioration in performance might be expected if leakage were present.

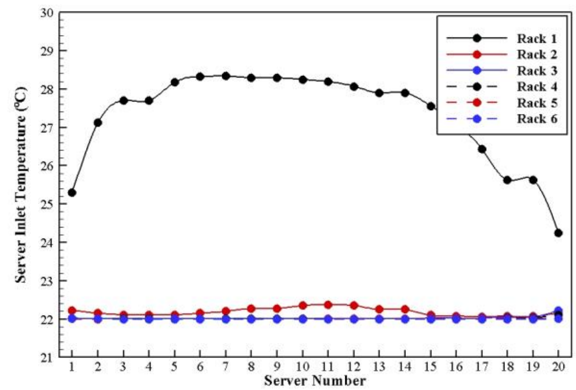

Figure 7. Air temperature at the inlet of servers with tiles of type An installed in the open aisle system, no UCL.

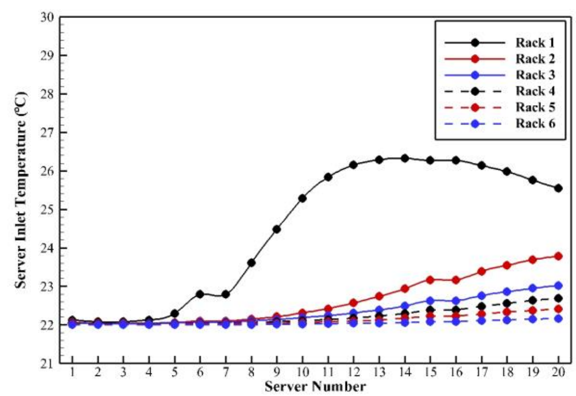

Figure 8. Air temperature at the inlet of servers with tiles of type B installed in the open aisle system, no UCL.

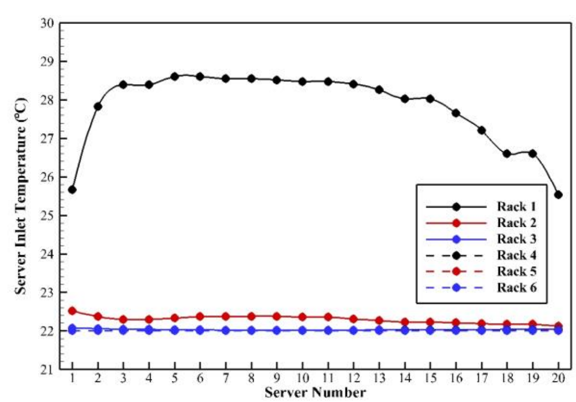

Figure 9. Air temperature at the inlet of servers with tiles of type C installed in the open aisle system, no UCL.

Figure 8 shows that the IAT of the servers at the bottom of the racks (server 1 in all the racks) is decreased by up to 2 °C when the under-cabinet gap was blocked. The overall maximum difference between IAT and SAT is 4.2 °C when tiles of type B are installed, which is similar to the results for case 1. This is because tile B directs the cooled air towards the face of the racks. So, even servers at the bottom of racks receive cold air directly from the adjacent tiles. The main reason of higher IAT in the servers of rack 1 in case 1 with tiles of type B installed was leakage of hot air from the entrance of aisle, not from the gap. Therefore, covering the under-cabinet gap has a minimal effect on the IAT of servers when tiles of type B were distributed in the aisle. In addition, by adjusting the angle of vanes of tile 1, more cooling air can be provided to the servers at the top half of rack 1, which can act as a barrier to the incoming hot air from the entrance of the aisle.

Figure 9 presents the IAT variation when tiles of type C were installed. Similar to type A, the IAT of servers in racks 2-6 is very close to SAT while, for the servers in rack 1, the IAT is between 3.5-6.6 °C higher than SAT. This close behavior is mainly because both of tiles A and C shoot air in a direction normal to the surface of the tile, and have relatively similar open area ratio. Finally, it is worthy to mention that placing the CRAH unit at the end of the hot aisle can facilitate hot air return with a minimum of air mixing with the cold aisle.

Case 3: CAC, with under-cabinet leakage

Installing CAC doors and ceiling can significantly eliminate the leakage of hot air from the top of the racks and the entrance of the aisle. However, the under-cabinet gap is often left uncovered in many data centers, which can be a source of air leakage. In case 3, the impact of tile design on the under-cabinet leakage and, consequently, IAT of servers is investigated. Figures 10-12 present the variation of IAT of servers when tiles of type A, B, and C are installed in the aisle, respectively. The IAT of servers when tiles of type A were installed are presented in Fig. 10. It is seen that the IAT of servers in the bottom half of the racks 2 to 6 is up to 3.1 °C higher than SAT. An interesting point is that IAT of the servers in rack 1 is equal to the SAT. This is because of the cold air leakage from CA to HA from beneath this rack that is shown in Fig. 14. This means that there is no hot air entering the cold aisle from the gap below rack 1. A similar behavior is seen when tiles of types B and C were installed in the aisle (see Figs. 11 and 12). When tiles of type A and C were installed (Figs. 10 and 12), the servers at the bottom of racks 3 and 4 are seen to have the maximum IAT and consequently are prone to overheating, while the maximum IAT were seen in racks 5 and 6 when tiles of type B were used. Therefore, placing high-density racks in the mentioned locations is not recommended in a similar configuration. In addition, over-provisioning of an aisle, with tiles of type A or C installed, results in jets of air with higher velocity above the tile that can lead to an enhanced hot air entrainment, which may worsen the situation.

Case 4: CAC, without under-cabinet leakage

By covering the under-cabinet gap in addition to installing CAC, and assuming that there is no leakage through the racks (perfect segregation), all of the possible paths of air leakage to the aisle are blocked. This simulation results showed that the IAT of all the servers is equal to SAT. Hence, the IAT results are not presented for the sake of space. The simulations showed that the maximum difference between outlet air temperatures (OAT) of servers is 0.6 °C. The OAT can be related to the airflow rate through equipment with the same IAT. A lower airflow rate results in higher OAT for a fixed heat dissipation. Here, the variation in OAT for equal IATs is due to the variation of pressure inside the CAC, which results in variation of airflow rates through different servers. It is worthy to remind, in this study, the airflow rate through IT units was linked with the pressure differential across the equipment by applying experimentally obtained effective flow curves as the inflow boundary condition.

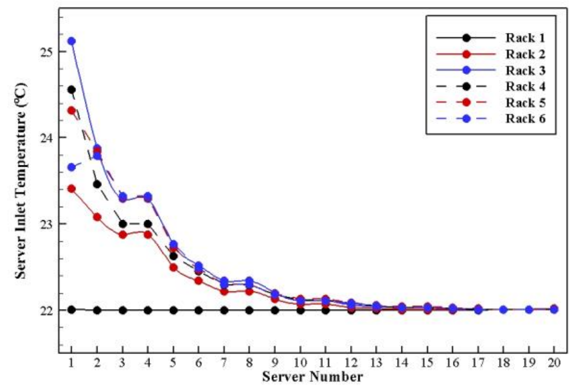

Figure 10. Air temperature at the inlet of servers with tiles of type A installed in the CAC system, with UCL.

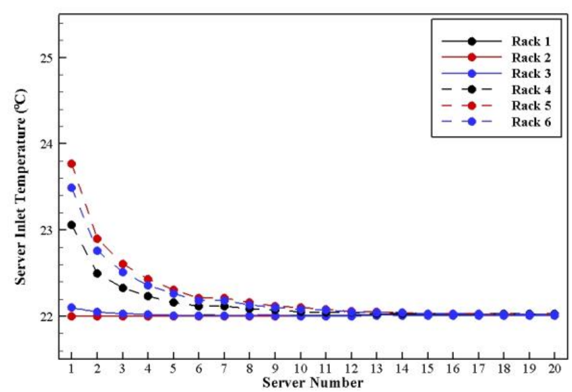

Figure 11. Air temperature at the inlet of servers with tiles of type B installed in the CAC system, with UCL.

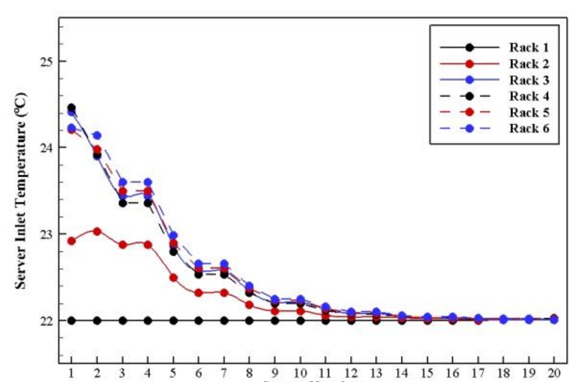

Figure 12. Air temperature at the inlet of servers with tiles of type C installed in the CAC system, with UCL.

Cases 5 and 6: Under-provisioned aisle

In cases 5 and 6, the under-provisioned scenarios of cases 3 and 4 are simulated, respectively. The CRAH was set to supply 10000 CFM airflow, which is about 83% provisioning. In case 5, the CAC was installed while the under-cabinet gap was not blocked. Therefore, hot air can leak to the cold aisle through this gap and mix with the supplied cold air. Figure 13 presents a comparison between averaged IATs of similarly-numbered IT equipment in all the racks (e.g. all the servers that are numbered 1). In this figure, unit 21 represents the network switches. For all types of tiles, the IAT of servers 1 (servers at the bottom of the racks, see Fig. 3) is at least 4.5 °C (up to 7.4 °C) higher than the SAT. This temperature rise is at least 3.4 °C for the first three servers at the bottom of the racks. This is due to UCL and its entrainment into supplied cold air from the tiles. With tiles of type B installed, it is seen that the average IAT of servers 1 is more than 2 °C higher than when other type of tiles were distributed. The supplied cooling air through tile B is angled so that jets of air hit the top half of server 2 and the servers above it. These jets of air act as a resistance to UCL to enter higher elevations. Hence, in case 5, the UCL is the main source of the air for servers 1 when tiles of type B are installed resulting in the highest temperature for Server 1 in contrast with the fully provisioned tests where type B provided the lowest temperatures.

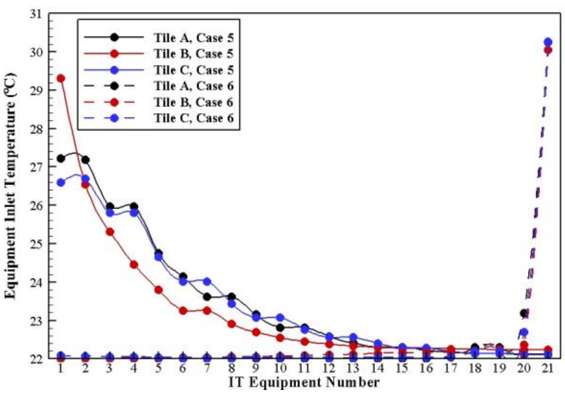

Figure 13. Averaged IATs of IT equipment at the same height, under-provisioned aisle.

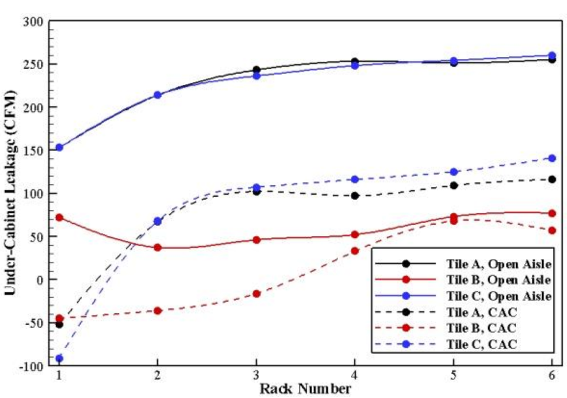

Figure 14. Under-cabinet leakage for the cases 1 and 3.

In case 6, the aisle was fully sealed. In this case, the IAT of servers 1-17 remains within 1 °C of SAT for all types of tiles. One important point in Fig. 13 is very high temperatures at the inlet of the network switches (more than 8 °C higher than SAT). The CFD simulation reveals that a reversed flow pulls hot air into the cold aisle through the network switches. The network switches are at the low end of the airflow and usually have the weakest air moving system among standard IT equipment. Therefore, the servers' fans pull air from the HA into the CA through network switches to make up for the shortage of supplied air due to the under-provisioning of the aisle. Consequently, the network switches are supplied with hot air from the HA, which puts them in danger of overheating. It should be mentioned that the IAT of network switches was very close to the SAT in cases 1 to 4.

Figure 14 presents the airflow rates through the under-cabinet gap that leak from the HA to the CA for the open and contained systems (cases 1 and 3). It shows that a reverse air leakage (from CA to HA) occurs beneath cabinet 1 for all tile types. Generally, the pressure behind the racks closer to the CRAH unit is less than that of the farther racks. This lower pressure can justify the reversed leakage from beneath rack 1. This reversed leakage also occurs for cabinets 2 and 3 when tiles of type B are installed, which is because tile B is a directional tile and directs the airflow toward the face of the racks. Consequently, a portion of the air can escape from the under-cabinet gap. Furthermore, this figure shows that the amounts of under-cabinet leakage in the open aisle system are higher than that of the contained configuration with the same type of tile. This leakage when tiles of type A and C are installed is up to 5 times greater than when tiles of type B are distributed in the aisle, which is mainly because of the lower openness of tiles of type A and C that results in jets of air with higher velocity above them. This high velocity creates a low-pressure area above the tile that can pull air from HA to CA. Another interesting point is that the magnitude of under-cabinet leakage in the open system when tile B is installed is less than that of the contained configuration when tiles of type A and C are installed.

A comparison between averaged IATs of servers of the same height in open and contained systems is presented in Figs. 15 and 16. In order to plot these figures, the average IAT of servers with the same number (e.g. all the servers that are numbered 1) in racks 1 to 6 was calculated. Figure 15 presents the averaged IATs of servers for cases 1 and 3 (open and contained aisles with UCL). The impact of tile design on the IAT of servers is clear in this figure. One interesting point is that the IAT of servers when tiles of type B were distributed in the open aisle is close to that of the CAC system with tiles of type A and C installed (less than 1.5 °C difference).

A similar comparison between cases 2 and 4 is presented in Fig. 16. In this figure, all the servers of case 4 have an IAT of 22 °C. In other words, the tile design is seen to have no impact on the IAT of servers in the fully-sealed aisle. Also, it can be inferred that the maximum difference between the average IAT of servers with and without CAC is about 1 °C, in this study.

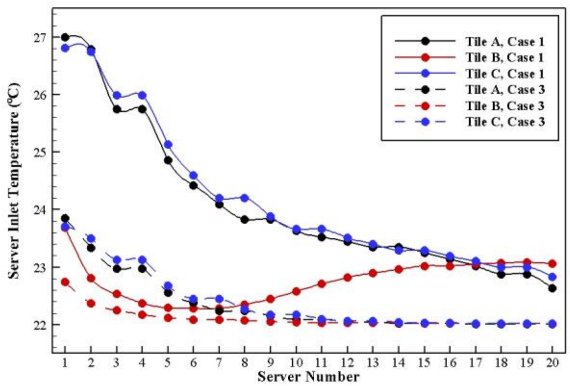

Figure 15. Averaged IATs of servers at the same height with UCL.

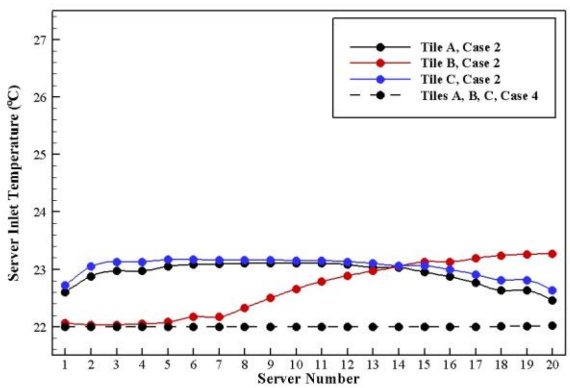

Figure 16. Averaged IATs of servers at the same height, no UCL.

Based on ASHRAE TC 9.9 guidelines [20], the majority of networking equipment has a typical maximum temperature rating of 40 or 45 °C. Therefore, even in the case of the reverse flow in the under-provisioned scenario, the IAT of network switches was still under the maximum temperature rating. However, there is a hidden danger that can be very hazardous to the equipment. A network switch can remain operational when it is supplied with enough air at the maximum allowed temperature, but it may fail when it is supplied with a low airflow rate at a much lower temperature than the maximum design temperature.

In a provisioned case, all units receive their required airflow rate. As the supply airflow rate decreases (under-provisioned case), the airflow through the equipment becomes less than the free delivery (FD) point since there is no air leakage into the CAC system to make up for the shortage of cooling air. Alissa et al. [22] showed that the airflow rate through an IT unit becomes zero at a critical differential backpressure, which is a characteristic of the unit. Therefore, for any CAC system, there is a critical under-provisioning point after which some of the equipment with a weaker airflow system are incapable of pulling air through. In this situation, there is a very low airflow rate for cooling of the equipment that leads to overheating of the unit. The switches are the most susceptible IT equipment to no- or low-flow situations and overheating due to their weak airflow system. Here, we propose a method for the calculation of an estimate of airflow rate associated with the critical under-provisioning as follows:

$$Q_c = N_{S_A} \times Q_{S_A @ pc_{NS}} + N_{S_B} \times Q_{S_B @ pc_{NS}} + \cdots - Q_{L @ pc_{NS}} \tag{1}$$

where Q_c is the critical under-provisioning airflow rate, N_{S_X} is the number of servers of type X and $Q_{S_X @ pc_{NS}}$ is the flow rate of server type X under differential pressure pc_{NS}, which is the critical pressure for the network switch or the IT equipment that has the weakest airflow system. The last term of Eq. (1), Q_L, is the leakage airflow rate into the aisle under differential pressure pc_{NS}, and can be used when air leakage into the aisle is not negligible.

By using Eq. (1), Q_c is calculated as 10554 CFM for the system presented in case 6 (12% under-provisioning). By applying the calculated Q_c as the CRAH supply airflow rate, CFD simulation reveals that the average airflow rate through the network switches is about 1 CFM, which is a very low airflow rate for cooling of a network switch. In this case, the mean airflow rate through the servers was decreased by about 10% when the mean airflow through the network switches was decreased by about 96%. This shows that Eq. (1) can be used for approximation of critical under-provisioning airflow rate. Also, it was seen that by decreasing the supply airflow rate by 8%, the airflow rate through the switches decreases by 50%.

Pressure Distribution at the Face of Racks

Figures 17 and 18 present pressure contours at the face of the racks in case 4. Because tile A has smaller openings (slots), the average velocity of resultant jets are higher that leads to a low local pressure above the tile. A local negative pressure decreases the flow rate through the corresponding server. Furthermore, the negative pressure can pull hot air from HA to CA if the cabinets are not sealed. On the other hand, tile B has larger openings and shoots the air toward the racks' faces. Therefore, lower jet velocities along with impingement of flow on the racks' surfaces result in higher pressure at the bottom of racks' surfaces. By comparing pressure contours in Figs. 17 and 18, it is seen that the local negative pressure can occur at the bottom, middle, or top of the racks' faces and, consequently, decrease the airflow rate through the corresponding IT equipment.

Recently, pressure has been introduced as an important control parameter for Data Center Infrastructure Management (DCIM) systems. Figures 17 and 18 also reveal that the pressure distribution inside a CAC system is not uniform and highly depends on the type of installed tiles. Hence, sufficient thought should be given to choosing the location and number of pressure sensors of a DCIM system by performing descriptive CFD simulations. The pressure contour when tiles of type C are installed is similar to that seen in Fig. 17 for the tiles of type A.

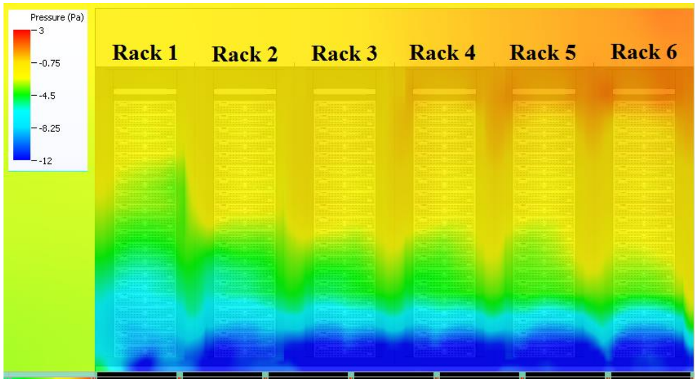

Figure 17. Pressure contour at the racks' faces when tiles of type A are installed, Case 4 (fully sealed CAC).

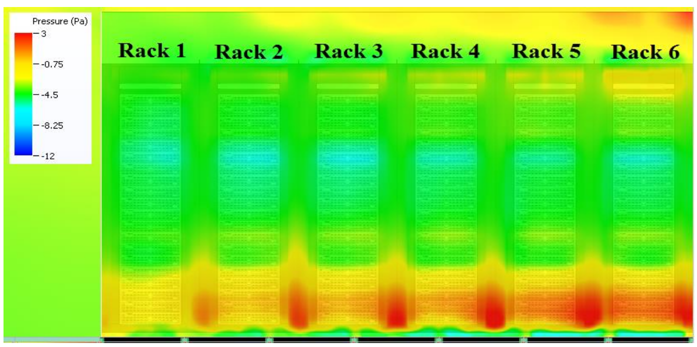

Figure 18. Pressure contour at the racks' faces when tiles of type B are installed, Case 4 (fully sealed CAC).

CONCLUSION

In this study, the impact of tile design on the inlet air temperature (IAT) of IT equipment in open and enclosed aisle configurations was studied. Experimentally validated geometrical resolution models of three different types of tiles were used to study six numerical scenarios. The investigated scenarios include open and contained cold aisle with open and covered under cabinet gap in neutrally provisioned and under-provisioned cases. Tile A is a slotted grill with understructure scoops, tile B is a directional grill and tile C is an axisymmetric perforated tile.

This study illustrated in the neutrally provisioned case the impact of tile design is significant in an open aisle while it has a minimal impact in a fully-sealed CAC system. It is seen that installing a directional tile like tile B can decrease the IAT of majority of servers in all the studied cases. As it was expected, installing a CAC system results in a notable drop in the IAT of servers. However, in an under-provisioned aisle, in contrast to the neutrally provisioned case, tile B resulted in the highest inlet temperature for Server 1 at the bottom of the racks when the under-cabinet gap was not covered. It is also shown that an under-provisioned fully sealed CAC system is prone to a danger of no/low-flow through the IT equipment with weaker air handling system. In addition, design of tile can significantly change the amount and behavior of UCL. Also, the results showed the elimination of hot air leakage to the CA may not be guaranteed by neutrally-provisioning or slightly over-provisioning of a CAC system. In addition, it was seen employing directional tiles (type B) can significantly reduce the air leakage through under-cabinet gap. It was found that the IAT of the majority of servers in the neutrally-provisioned open aisle can be moved to within 2 °C of SAT by covering the under-cabinet gap. Therefore, for the scenarios studied, installing the proper type of tile can be suggested as an alternative solution to the CAC when there are limitations such as fire suppression systems that present challenges to enclosing the aisle. Furthermore, since the velocity of air jets above the tile has a significant impact on the UCL and the bypass of air from the top of the racks, the openness of tiles should be chosen thoughtfully to avoid excess mix of hot and cold air.

The results showed that the biggest impact of CAC enclosure installation on the IAT of servers is on the racks at the entrance of the aisle. It should be mentioned that even though it was shown that the type of tile has a minimal effect on the IAT of servers in the fully sealed CAC system, the impact of the tile design can be considerable in an aisle that is populated by IT equipment with different required cooling airflow rate or IT load in each aisle. In addition, the results showed that the hot air leakage to CA through the under-cabinet gap increases with the distance from CRAH unit. The simulations showed that a reverse leakage (from CA to HA) is present under the cabinets closer to the CRAH unit. Consequently, some hot air must leak into the cold aisle to make up for the reverse leakage. It means that hot air can leak into the CA although it is neutrally-provisioned.

This study also demonstrates that the pressure distribution inside a CAC system can be non-uniform and it depends on the design of the perforated tiles. Hence, the type of tile should be considered in selection of the location and number of pressure sensors of a DCIM system. Furthermore, it is shown that a completely sealed CAC system is prone to a hidden danger of overheating in equipment with weaker airflow systems (such as network switches) when the CA is under-provisioned. Only a few percentage points of under-provisioning can lead to a no- or low-flow condition in the network switches. Finally, a predictive equation for the critical under-provisioning point as a function of the experimental characteristics of IT equipment is presented. To avoid the low-flow situation, implementation of a pressure relief valve can be suggested to let the air leak into the cold aisle in case of negative pressure differential build up. This leakage may incrementally increase the IAT of equipment by a few degrees but provides sufficient airflow for the IT units. Another solution can be mounting of half-depth network switches to the back-rack flanges to assure they have access to sufficient airflow.

ACKNOWLEDGMENTS

The authors would like to thank Dr. K. Ghose, U. L. N. Puvvadi and K. D. Hall from Binghamton University Computer Science and Data Center Group. We would also like to thank the ES2 partner universities for their support and advice. This work is supported by NSF IUCRC Award No. IIP-1134867 and MRI Award No. CNS1040666.

REFERENCES

[1] Kang, S., Schmidt, R., Kelkar, K. M., Radmehr, A. and Patankar, S. V., 2000, “A methodology for the design of perforated tiles in raised floor data centers using computational flow analysis,” The Seventh Intersociety Conference on Thermal and Thermomechanical Phenomena in Electronic Systems (ITherm), Las Vegas, Nevada, pp. 215–224.

[2] Schmidt, R. R., Karki, K. C., Kelkar, K. M., Radmehr, A. and Patankar, S. V., 2001, “Measurements and predictions of the flow distribution through perforated tiles in raised-floor data centers,” IPACK2001-15728, The Pacific Rim/ASME International Electronic Packaging Technical Conference and Exhibition, Kauai, Hawaii, pp. 1-10.

[3] VanGilder, J. W. and Schmidt, R. R., 2005, “Airflow uniformity through perforated tiles in a raised-floor data center,” IPACK2005-73375, ASME 2005 Pacific Rim Technical Conference and Exhibition on Integration and Packaging of MEMS, NEMS, and Electronic Systems collocated with the ASME 2005 Heat Transfer Summer Conference, San Francisco, CA, pp. 493–502.

[4] Ling, Y.-Z., Zhang, X.-S., Zhang, K. and Jin, X., 2017, “On the characteristics of airflow through the perforated tiles for raised-floor data centers,” J. Build. Eng., 10, pp. 60–68.

[5] Arghode, V. K., Kang, T., Joshi, Y., Phelps, W. and Michaels, M., 2017, “Measurement of Air Flow Rate Through Perforated Floor Tiles in a Raised Floor Data Center,” J. Electron. Packag., 139, pp. 11007.

[6] Karki, K. C. and Patankar, S. V., 2006, “Airflow distribution through perforated tiles in raised-floor data centers,” Build. Environ., 41, pp. 734–744.

[7] Patankar, S. V., 2010, “Airflow and Cooling in a Data Center,” J. Heat Transfer 132, pp. 73001.

[8] Alkharabsheh, S., Fernandes, J., Gebrehiwot, B., Agonafer, D., Ghose, K., Ortega, A., Joshi, Y. and Sammakia, B., 2015, “A Brief Overview of Recent Developments in Thermal Management in Data Centers,” J. Electron. Packag., 137, pp. 40801.

[9] Abdelmaksoud, W.A., Khalifa, H.E., Dang, T.Q., Elhadidi, B., Schmidt, R.R. and Iyengar, M., 2010, “Experimental and computational study of perforated floor tile in data centers,” 12th IEEE Intersociety Conference on Thermal and Thermomechanical Phenomena in Electronic Systems (ITherm), Las Vegas, NV, pp. 1–10.

[10] Arghode, V. K., Kumar, P., Joshi, Y., Weiss, T. and Meyer, G., 2013, “Rack Level Modeling of Air Flow Through Perforated Tile in a Data Center,” J. Electron. Packag., 135, pp. 30902.

[11] Arghode, V. K., Woodruff, G. W. and Joshi, Y., 2016, “Modified Body Force Model for Air Flow through Perforated Floor Tiles in Data Centers,” J. Electron. Packag., 138, pp. 31002.

[12] Joshi, Y. and Kumar, P., 2012, Energy efficient thermal management of data centers, Springer, New York.

[13] U.S. Briefing., 2013, “International Energy Outlook 2013”, US Energy Inf. Adm., Washington, DC.

[14] Bharath, M., Shrivastava, S. K., Ibrahim, M., Alkharabsheh, S. A. and Sammakia, B. G., 2013, “Impact of Cold Aisle Containment on Thermal Performance of Data Center,” IPACK2013-73201, International Technical Conference and Exhibition on Packaging and Integration of Electronic and Photonic Microsystems, Burlingame, CA, pp. 1–5.

[15] Makwana, Y. U., Calder, A. R. and Shrivastava, S. K., 2014, “Benefits of properly sealing a cold aisle containment system”, IEEE Intersociety Conference on Thermal and Thermomechanical Phenomena in Electronic Systems (ITherm), Orlando, FL, pp. 793–797.

[16] Alissa, H. A., Nemati, K., Sammakia, B. G., Seymour, M. J., Tipton, R., Mendo, D., Demetriou, D. W., and Schneebeli, K., 2016, “Chip to Chiller Experimental Cooling Failure Analysis of Data Centers: The Interaction Between IT and Facility,” IEEE Trans. Components, Packag. Manuf. Technol., 6, pp. 1361–1378.

[17] Shrivastava, S. K. and Ibrahim, M., 2013, “Benefit of Cold Aisle Containment During Cooling Failure,” IPACK2013-73219, International Technical Conference and Exhibition on Packaging and Integration of Electronic and Photonic Microsystems, Burlingame, CA, pp. V002T09A021.

[18] Khalili, S., Alissa, H. A., Tradat, M. I., Nemati, K., Sammakia, B., Seymour, M., 2017, “Experimental Methods to Characterize the Impact of Cross Flow Orientation on Jets of Air after a Perforated Tile,” Thermal Measurement, Modeling & Management Symposium (SEMI-THERM), San Jose, CA, pp. 163–171.

[19] Alissa, H.A., Nemati, K., Sammakia, B., Seymour, M., Schneebeli, K. and Schmidt, R., 2015, “Experimental and numerical characterization of a raised floor data center using rapid operational flow curves model,” IPACK2015-48234, International Technical Conference and Exhibition on Packaging and Integration of Electronic and Photonic Microsystems, San Francisco, CA, pp. V001T09A016.

[20] ASHRAE Technical Committee, 2011, “Thermal Guidelines for Data Processing Environments,” Am. Soc. Heating, Refrig. Air-Conditioning Eng. Inc, pp. 1–45.

[21] Arghode, V. K. and Joshi, Y., 2013, “Modeling strategies for air flow through perforated tiles in a data center,” IEEE Trans. Components, Packag. Manuf. Technol., 3, pp. 800–810.

[22] Alissa, H. A., Nemati, K., Sammakia, B. G., Schneebeli, K., Schmidt, R. and Seymour, M. J., 2016, “Chip to Facility Ramifications of Containment Solution on IT Airflow and Uptime,” IEEE Trans. Components, Packag. Manuf. Technol., 6, pp. 67–78.

